International Journal of Heat and Mass Transfer 52 (2009) 232–238

Contents lists available at ScienceDirect

International Journal of Heat and Mass Transfer

journal homepage: www.elsevier.com/locate/ijhmt

The functional identification approach for numerical reconstruction of the temperature-dependent thermal-conductivity coefficient

V.T. Borukhov *, V.A. Tsurko, G.M. Zayats

Institute of Mathematics, National Academy of Sciences of Belarus, Minsk 220072, Belarus

ARTICLE INFO

Article history:
Received 4 December 2007
Available online 8 August 2008

Keywords:
Nonlinear heat-conduction equation
Thermal-conductivity coefficient
Inverse problem
Functional identification
Numerical simulation

ABSTRACT

The functional identification approach of the thermal-conductivity coefficient for the unsteady-state nonlinear heat-conduction equation is considered. Unlike traditional methods, the proposed algorithm does not utilize approximations of the coefficient with the aid of the specified system of basis functions. The results of computational experiments are presented.

1. Introduction

The problems of the reconstruction of the thermal-conductivity and diffusion coefficients of nonlinear media are of interest in creating modern technologies of producing various materials. These problems fall into the class of inverse problems of mathematical physics. The scientific trend associated with the theory and practice of solving nonlinear inverse heat-conduction problems takes its origin at the middle of the second half of the 20th century [1–16]. The present-day development of this trend is stimulated by:

- the need in reliable reconstruction of thermal-conductivity coefficients of complex structure [2,7,10–12],
- the search for sufficient conditions of the solvability of inverse heat-conduction problems that are close to the needed conditions [13,14].

We note that the reconstruction of the coefficients of a complex structure whose plots have, for example, breakpoints are of importance for investigation of phase transitions. The conditions of the uniqueness of the solution of an inverse problem are important in planning physical experiments on determining the characteristics of materials.

At the present time, in numerical solution of inverse problems in the mathematical physics, various methods of the minimization of objective functionals are widely applied. In particular, the regularizing properties of the conjugate gradient method are well known [1,2]. The constituent part of this method applied to the problem of identification of the thermal-conductivity coefficient $\lambda(T)$ is computations of the values of the operator conjugate to the inner superposition operator. The standard approach to such computations is associated with the change of variables in the double integral, which leads to a complex and hard-to-control numerical procedure. In view of this, in many publications (see, e.g. [2,3,7,12,15,16]), the finite-dimensional approximation of sought coefficients was considered. Thereby the initial, functional, and consequently, infinite-dimensional problem was interpreted in these works as a finite-dimensional one. Inherent in such an approach is both certain advantages associated with the regularizing properties of finite-dimensional approximations and disadvantages due to the prior uncertainty in the selection of basis functions of approximation and of their number.

In [5,7,8], a functional approach not requiring preliminary finite-dimensional representation of the sought coefficient is presented. The authors note the limitations of their approach associated with the requirement of the solvability of the special functional equation at each step of the iteration process.

In [9], a new approach of the functional identification of the thermal-conductivity coefficient was suggested. In this approach, the scheme of gradient methods of minimization of the objective functional is used without preliminary finite-dimensional approximation of the sought coefficient and without requirements of the solvability of functional equations. This has become possible by virtue of the new integro-differential representations obtained in [9] for the operator conjugate to the inner superposition operator

* Corresponding author.
E-mail addresses: borukhov@im.bas-net.by (V.T. Borukhov), vtsurko@im.bas-net.by (V.A. Tsurko), zayats@im.bas-net.by (G.M. Zayats).

0017-9310/$ - see front matter © 2008 Elsevier Ltd. All rights reserved.
doi:10.1016/j.ijheatmasstransfer.2008.01.043

Nomenclature

b	length of space segment
$c(T)$	heat-capacity coefficient
G	domain of definition of objective functional
h	step in spatial grid
t	time
t_f	final instant of time
$T(x,t)$	temperature
w_x	spatial grid
w_t	time grid
w_T	temperature grid
x	spatial coordinate
x_*	point of temperature measurement
$\|\cdot\|$	norm in the space $L_2[T^{(1)},T^{(2)}]$ or $W_2^1[T^{(1)},T^{(2)}]$
β	coefficient of descent
$\lambda(T)$	thermal-conductivity coefficient
$\lambda_0(T)$	initial approximation
$\lambda_n(T)$	nth approximation
$\lambda_m(T)$	model function
ε	tolerance
τ_t	step in time grid
τ_T	step in temperature grid
Ω	domain of definition

Subscripts

m	model
T	temperature

not associated with change of variables in double integrals. In [9], various variants of the functional identification of the thermal-conductivity coefficient are considered. They differ in the selection of functional space and of the corresponding Hilbert norm for the function $\lambda(T)$. Work [10] is devoted to numerical realization of the method of functional identification. The work also considers some qualitative properties of the variants of functional identification. In particular, the boundary effects appearing on reconstruction of coefficients by the method of functional identification and associated with that or other choice of the Hilbert norm of coefficients in the Sobolev spaces are noted in [10]. The numerical stability of algorithms in a wide range of perturbations of the input data of an inverse problem is noted.

This work presents the investigations that were begun in [9,10]. Here, we present a brief description of the algorithmic part of the functional identification approach and in Appendix A gives difference schemes for linear and nonlinear unsteady-state initial boundary-value problems being a constituent part of the scheme of conjugate gradients for reconstruction of the thermal-conductivity coefficient in a nonlinear unsteady-state heat-conduction equation. We discuss the problems of organization of the computational process and consider the results of computational experiments.

2. Statement of the problem

In the domain $\Omega = \{(x,t) : 0 < x < b,\ 0 < t \leqslant t_f\}$, we will consider the nonlinear parabolic equation

$$c(T)\frac{\partial T}{\partial t} = \frac{\partial}{\partial x}\left(\lambda(T)\frac{\partial T}{\partial x}\right) \tag{1}$$

with the initial conditions

$$T(x,0) = \overline{T}(x), \quad x \in (0,b), \tag{2}$$

and boundary-value conditions

$$T(0,t) = g_1(t), \quad T(b,t) = g_2(t), \qquad t \in [0,t_f]. \tag{3}$$

The initial and boundary-value conditions are consistent, $c(T)$, $\lambda(T)$, $\overline{T}(x)$, $g_1(t)$ and $g_2(t)$ are given functions.

Problems (1)–(3) describe the processes of heat transfer, diffusion, and filtration in nonlinear media. In what follows, for the sake of definiteness, we will assume that conditions (1)–(3) describe the process of heat transfer. A direct problem for finding the function $T(x,t)$ is formulated in the form of Eqs. (1)–(3). The methods of solving the given direct heat-conduction problem, both analytical [17] and numerical ones [18], are well known.

We will consider an inverse problem in which along with $T(x,t)$ the thermal-conductivity coefficient $\lambda(T)$ is also unknown. The solution of such a problem can be found from conditions (1)–(3) and from the additional condition

$$T(x_*,t) = \widetilde{T}(t), \quad x_* \in (0,b), \quad \forall t \in [0,t_f], \tag{4}$$

where x_* is the fixed point at which temperature is measured.

The present statement of the inverse problem is a classical one. Methodically the solvability of this problem is based on the well-known results obtained by Muzylev, Klibanov, and Alifanov et al. (the review of these results is given in [2,6,7,11]), from which the existence and uniqueness of problem solution with additional limitations on the input data $c(T)$, $\overline{T}(x)$, $g_1(t)$, $g_2(t)$, and $\widetilde{T}(t)$ follow. In particular, apart from the standard requirement of positiveness, continuity, and piecewise differentiability of the function $c(T)$ for the uniqueness of the solution it is sufficient to require that the following conditions be satisfied: $\overline{T}(x) = \text{const}$, $g_1(t)$, $g_2(t)$, $\widetilde{T}(t)$ are monotonically increasing functions.

3. Algorithm

We propose the iterative algorithm for minimization of the objective functional:

$$J(\lambda) = \int_0^{t_f}\left(T(x_*,t) - \widetilde{T}(t)\right)^2 \mathrm{d}t. \tag{5}$$

Following [9,10], we consider three variants of the algorithm, marking them with the index $i = 1,2,3$. In the first of them ($i = 1$), we assume that the domain, G, of the functional J coincides with some open set in the Hilbert space, $L_2[T^{(1)},T^{(2)}]$, of square integrable functions with the norm,

$$\|\lambda\|_{i=1} = \left(\int_{T^{(1)}}^{T^{(2)}}(\lambda(\xi))^2\,\mathrm{d}\xi\right)^{\frac{1}{2}}, \tag{6}$$

where $T^{(1)} = \min_{(x,t)\in\overline{\Omega}}T(x,t)$ and $T^{(2)} = \max_{(x,t)\in\overline{\Omega}}T(x,t)$. For $i = 2,3$, the domain G coincides with an open set in the Sobolev space of absolute integrable functions, $W_2^1[T^{(1)},T^{(2)}]$. When $i = 2$, the norm is defined as

$$\|\lambda\|_{i=2} = \left(\left(\lambda\left(T^{(1)}\right)\right)^2 + \int_{T^{(1)}}^{T^{(2)}}\left(\frac{\mathrm{d}\lambda(\xi)}{\mathrm{d}\xi}\right)^2\mathrm{d}\xi\right)^{\frac{1}{2}}, \tag{7}$$

and when $i = 3$, it is defined by

$$\|\lambda\|_{i=3} = \left(\left(\lambda\left(T^{(2)}\right)\right)^2 + \int_{T^{(1)}}^{T^{(2)}} \left(\frac{\mathrm{d}\lambda(\xi)}{\mathrm{d}\xi}\right)^2 \mathrm{d}\xi \right)^{\frac{1}{2}}. \quad (8)$$

These three algorithms' variants differ from each other by the quality of approximations of the function $\lambda(T)$ in the boundary points $\lambda(T^{(1)})$ and $\lambda(T^{(2)})$. Moreover, the variants II and III have a strong smoothing property. On the other hand, the variant I allows us to restore the function $\lambda(T)$ in the neighborhood of the breakpoints of a plot $\lambda(T)$ almost without any lost of accuracy. The properties of the algorithm are described in detail in Appendix A and in the paper [10].

The algorithm of the functional identification of the inverse problems (1)–(4) is describes as follows. The initial input data constitute the initial approximation $\lambda_0(T)$ to the function $\lambda(T)$ along with the data $\widetilde{T}(t)$ measured at the fixed point x_* at any time $t \in [0, t_f]$ and the null values of l_{-1} (see Eq. (10)). The output data on nth + 1 iteration step are two functions, $l_n(T)$ and $\lambda_{n+1}(T)$, that are obtained from the vector recursive relations:

$$\lambda_{n+1}(T) = \lambda_n(T) - \beta_n l_n(T), \qquad n \in \{0,1,2,\ldots\}, \quad \lambda_0 \text{ is given}, \quad (9)$$

$$l_n(T) = J^i_{\lambda_n}(T) + \gamma^i_{n-1} l_{n-1}(T), \qquad n \in \{0,1,2,\ldots\}, \quad l_{-1} = 0, \quad (10)$$

where $\lambda_{n+1}(T)$ is the nth + 1 approximation to $\lambda(T)$, $l_n(T)$ is the direction of descent on the nth + 1 iteration, parameters β_n, γ^i_{n-1}, and $J^i_{\lambda_n}$ are defined by the relations (13)–(20). The flow-chat of the nth + 1 iteration is schematically presented in Fig. 1. The recurrence relations (9) and (10) are an essential part of the conjugate gradient method [2,9]. The iteration is stopped when

$$\int_0^{t_f} p_n(t)^2 \,\mathrm{d}t \leqslant \varepsilon, \quad p_n(t) = T_n(x_*, t) - \widetilde{T}(t), \quad (11)$$

where ε is the tolerance, and $T_n(x,t)$ is the solution of the following initial boundary value problem:

$$\begin{aligned} &c(T_n)\frac{\partial T_n}{\partial t} = \frac{\partial}{\partial x}\left(\lambda_n(T_n)\frac{\partial T_n}{\partial x}\right), \quad (x,t) \in \Omega, \\ &T_n(x,0) = \overline{T}(x), \ \ x \in (0,b), \quad T_n(0,t) = g_1(t), \\ &T_n(b,t) = g_2(t), \ \ t \in [0,t_f]. \end{aligned} \quad (12)$$

Selection of the tolerance ε is based on the discrepancy principle and generalized discrepancy principle, described in detail in [2]. We should note that it is helpful to renew the iteration procedures (9) and (10) in the case of increasing of the objective functional (5) on nth + 1 iteration. In this case, we choose the initial approximation as $\lambda_0(T) = \lambda_n(T)$.

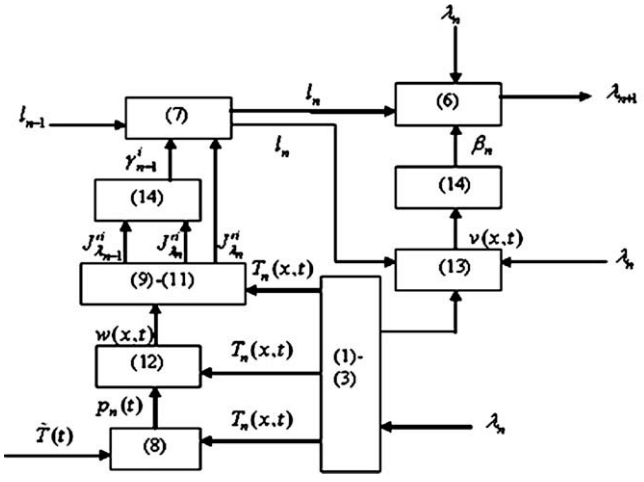

Fig. 1. Scheme of finding $\lambda_{n+1}(T)$ from the known values of $\lambda_n(T)$ and $l_n(T)$.

Now we are going to describe the algorithm of determination of parameters β_n, γ^i_{n-1}, and $J^i_{\lambda_n}$. The function $J^i_{\lambda_n}$ is the gradient of the functional (5) at the point $\lambda = \lambda_n$ and it is calculated according to the procedure described in [9,10] for each variant $i \in \{1,2,3\}$ according to one of the following formulas:

$$\begin{aligned} J^i_{\lambda_n}|_{i=1} &= -\frac{\mathrm{d}}{\mathrm{d}z}\int_0^b \int_0^{t_f} \chi(z, T_n(x,t)) \frac{\partial T_n(x,t)}{\partial x}\frac{\partial w_n(x,t)}{\partial x}\,\mathrm{d}t\,\mathrm{d}x \\ &\equiv -\frac{\mathrm{d}}{\mathrm{d}z}\int_\Omega R(z,x,t)\frac{\partial T_n(x,t)}{\partial x}\frac{\partial w_n(x,t)}{\partial x}\,\mathrm{d}x\,\mathrm{d}t, \end{aligned} \quad (13)$$

$$\begin{aligned} J^i_{\lambda_n}|_{i=2} = &-\int_\Omega \frac{\partial T_n(x,t)}{\partial x}\frac{\partial w_n(x,t)}{\partial x}\,\mathrm{d}x\,\mathrm{d}t \\ &-\int_{T^{(1)}}^{z}\int_\Omega r(\tau,x,t)\frac{\partial T_n(x,t)}{\partial x}\frac{\partial w_n(x,t)}{\partial x}\,\mathrm{d}x\,\mathrm{d}t\,\mathrm{d}\tau, \end{aligned} \quad (14)$$

$$\begin{aligned} J^i_{\lambda_n}|_{i=3} = &-\int_\Omega \frac{\partial T_n(x,t)}{\partial x}\frac{\partial w_n(x,t)}{\partial x}\,\mathrm{d}x\,\mathrm{d}t \\ &-\int_{z}^{T^{(2)}}\int_\Omega R(\tau,x,t)\frac{\partial T_n(x,t)}{\partial x}\frac{\partial w_n(x,t)}{\partial x}\,\mathrm{d}x\,\mathrm{d}t\,\mathrm{d}\tau. \end{aligned} \quad (15)$$

Here

$$\chi(z,s) = \begin{cases} 1, & \text{if} \quad T^{(1)} \leqslant s \leqslant z, \\ 0, & \text{if} \quad z \leqslant s \leqslant T^{(2)}, \end{cases}$$

is the characteristic function of the set $\{s|T^{(1)} \leqslant s \leqslant z\}$; $R(z,x,t)$ and $r(z,x,t)$ are the characteristic functions of the sets $\Lambda(z) = \{(x,t) \in \Omega | T_n(x,t) \leqslant z \leqslant T^{(2)}\}$ and $\overline{\Lambda}(z) = \Omega \setminus \Lambda(z) = \{(x,t) \in \Omega | T^{(1)} \leqslant z \leqslant T_n(x,t)\}$, respectively.

The function $w_n = w_n(x,t)$ in formulas (13)–(15) is the solution of the following non-homogeneous initial boundary value problem:

$$\begin{aligned} &c(T_n)\frac{\partial w_n}{\partial t} + \lambda_n(T_n)\frac{\partial^2 w_n}{\partial x^2} - \delta(x - x_*)p_n(t) = 0, \quad (x,t) \in \Omega, \\ &w_n(x,t_f) = 0, \quad x \in (0,b), \qquad w_n(0,t) = w_n(b,t) = 0, \quad t \in [0,t_f], \end{aligned} \quad (16)$$

where $\delta(x - x_*)$ is Dirac's function. Note that formulas (13)–(15) follow from integro-differential representations of the operators conjugate to the inner superposition operator [9].

The parameter γ^i_{n-1} is the ratio of squares of two norms:

$$\gamma^i_{n-1} = \frac{\left\|J^i_{\lambda_n}\right\|^2}{\left\|J^i_{\lambda_{n-1}}\right\|^2}, \quad i = 1,2,3. \quad (17)$$

According to (6)–(8), the squares of these norms can be expressed as

$$\begin{aligned} &\left\|J^1_{\lambda_n}\right\|^2_{L_2} = \int_{T^{(1)}}^{T^{(2)}} (J^1_{\lambda_n})^2\,\mathrm{d}z, \\ &\left\|J^i_{\lambda_n}\right\|^2_{W_2^1} = \left(\int_\Omega \frac{\partial T_n(x,t)}{\partial x}\frac{\partial w_n(x,t)}{\partial x}\,\mathrm{d}x\,\mathrm{d}t\right)^2 + \int_{T^{(1)}}^{T^{(2)}} l^2_{n,i}\,\mathrm{d}z, \quad i = 2,3, \end{aligned} \quad (18)$$

where

$$\begin{aligned} l_{n,2} &= \int_\Omega r(\tau,x,t)\frac{\partial T_n(x,t)}{\partial x}\frac{\partial w_n(x,t)}{\partial x}\,\mathrm{d}x\,\mathrm{d}t, \\ l_{n,3} &= \int_\Omega R(z,x,t)\frac{\partial T_n(x,t)}{\partial x}\frac{\partial w_n(x,t)}{\partial x}\,\mathrm{d}x\,\mathrm{d}t. \end{aligned}$$

Finally, the parameter β_n is defined by the ratio of integrals:

$$\beta_n = \int_0^{t_f} p_n(s)v_n(x_*,s)\,\mathrm{d}s \Big/ \int_0^{t_f} v_n^2(x_*,s)\,\mathrm{d}s, \quad (19)$$

where the function $v_n = v_n(x,t)$ is the solution of the following initial boundary value problem:

$$\begin{aligned} &\frac{\partial}{\partial t}(c(T_n)v_n) = \frac{\partial^2}{\partial x^2}(\lambda_n(T_n)v_n) + \frac{\partial}{\partial x}\left(l_n(T_n)\frac{\partial T_n}{\partial x}\right), \quad (x,t) \in \Omega, \\ &v_n(x,0) = 0, \quad x \in (0,b), \\ &v_n(0,t) = v_n(b,t) = 0, \quad t \in [0,t_f]. \end{aligned} \tag{20}$$

The functional identification approach has been realized numerically. The solution of the initial boundary-value problems posed in this section can be found by the difference method [18]. The computation of integrals in Eqs. 13,14,15, (17) and (19) is based on the trapezium method [19]. Here, the derivatives with respect to the variable x in the integrands are replaced by difference relations of the second order of approximation. The description of numerical algorithms that implement the functional identification approach is given in Appendix A.

4. Numerical simulation

We will illustrate the operation of the numerical algorithms of the functional identification approach on model examples and give some of typical results of computational experiments.

Depending on the choice of the gradient $J^i_{\lambda_n}$ $(i = 1,2,3)$ (Eqs. (13)–(15)) recurrent relations (9) and (10) will be called algorithms I, II, and III, respectively.

Example 1. The form of the model function $\lambda(T) = \lambda_m(T)$ in problems (1)–(4) will be selected to be rather complex (see Figs. 3–5):

$$\lambda_m(T) = \begin{cases} 25.0\exp(T/450.0), & \text{if } T < 450\ ^\circ\text{C}, \\ 6.073\times10^{-4}(T-700.0)^2 + 30.0, & \text{if } 450\ ^\circ\text{C} \leqslant T < 900\ ^\circ\text{C}, \\ 9.025\times10^{-3}T + 46.17, & \text{if } T \geqslant 900\ ^\circ\text{C}. \end{cases} \tag{21}$$

The plots of the functions $c(T) = c_m(T)$ and $g_1(t) = g_2(t)$ are given in Fig. 2a and b, respectively. We assume that $b = 3.0$, $t_f = 2.0$, $\overline{T}(x) = 30.0$, and $x_* = 1.0$. As the approximation of the function $\widetilde{T}$, we take the numerical solution of the problems (1)–(3) at the point $x = x_*$, $\forall t \in [0,t_f]$ at $c(T) = c_m(T)$, $\lambda(T) = \lambda_m(T)$, obtained by the difference scheme (27) (see Appendix A) with small steps h_i and τ_t of grids ω_x (24) and ω_t (25) (see Appendix A).

Figs. 3–5 demonstrate the results of modeling of thermal-conductivity coefficient (21) by the functional identification approach. Fig. 3 depicts the results of the reconstruction of the coefficient

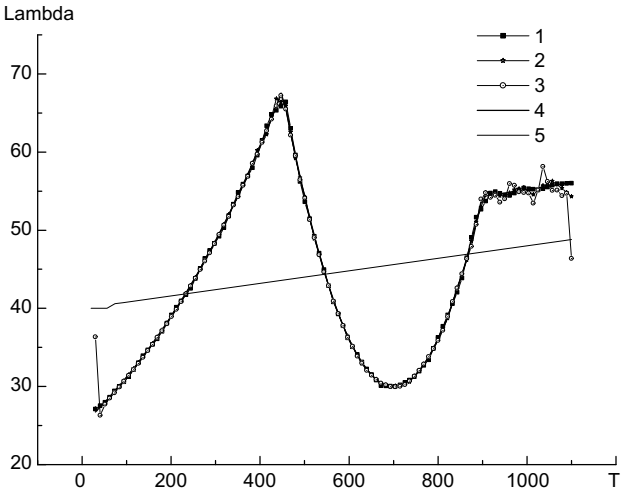

Fig. 3. Results of reconstruction of the coefficient $\lambda_m(T)$ according to algorithm I depending on the steps of numerical differentiation of the operator in (13): $\tau_T = 37.0$ (1); $\tau_T = 21.0$ (2); $\tau_T = 3.5$ (3); $\lambda_m(T)$ (4); and $\lambda_0(T)$ (5).

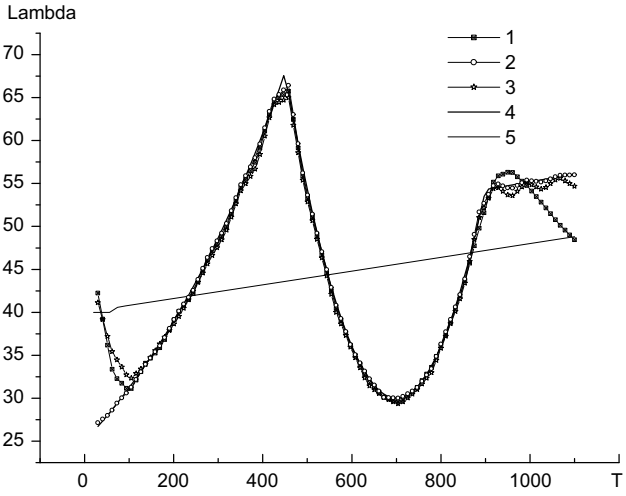

Fig. 4. Results of reconstruction of the coefficient $\lambda_m(T)$ according to algorithm I depending on the values of the point x_*: $x_* = 0.28$ (1); $x_* = 2.0$ (2); $x_* = 2.8$ (3); $\lambda_m(T)$ (4); and $\lambda_0(T)$ (5).

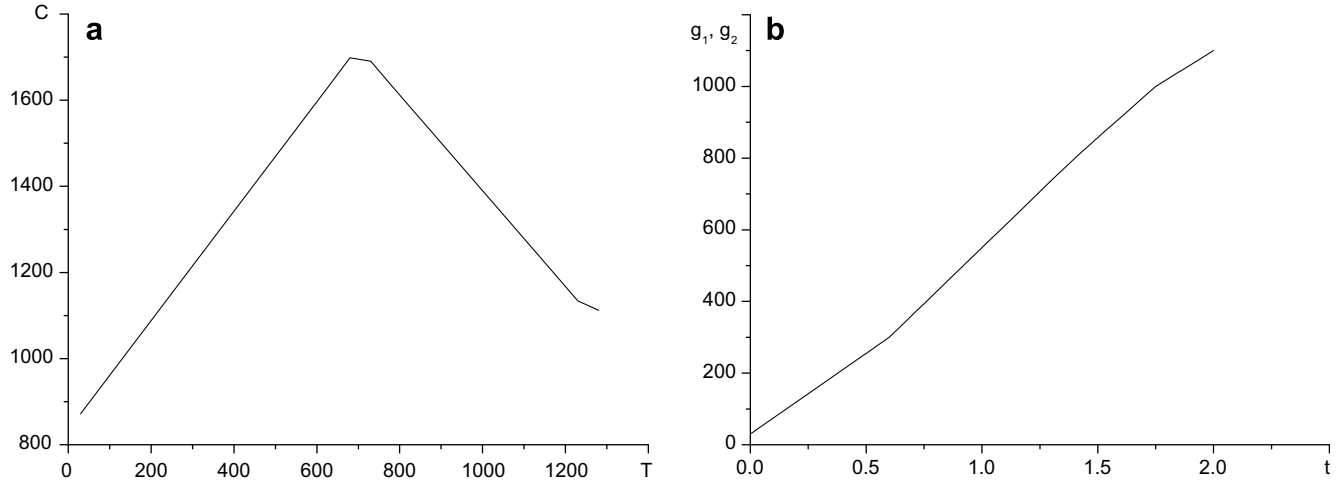

Fig. 2. Form of the function $c_m(T)$ (a) and functions $g_1(t) = g_2(t)$ (b).

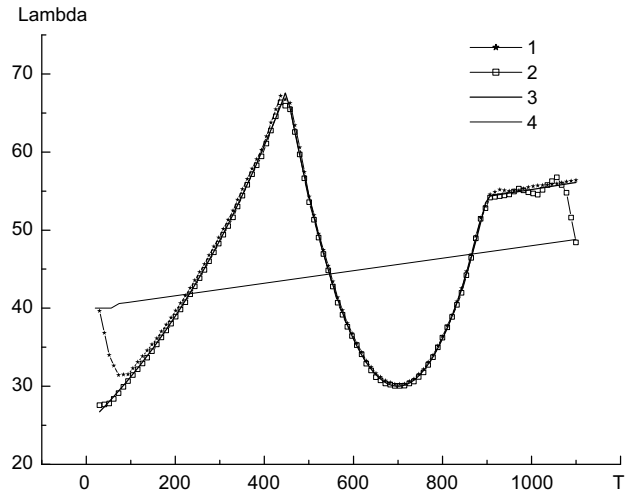

Fig. 5. Results of calculation of the coefficient $\lambda_m(T)$ according to algorithm II and III: (1) algorithm II; (2) algorithm III; (3) $\lambda_m(T)$; and (4) $\lambda_0(T)$.

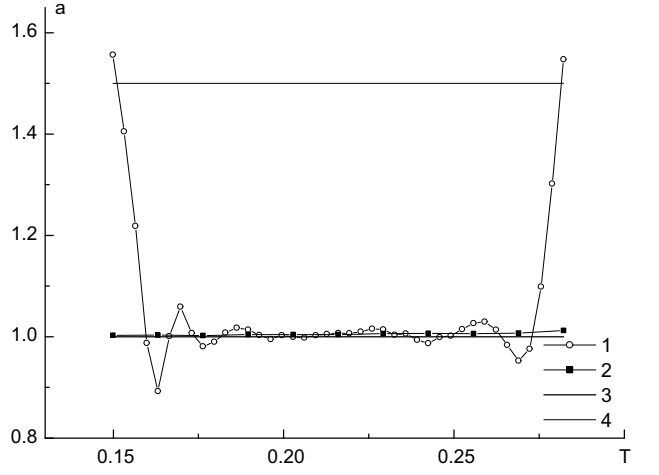

Fig. 6. Influence of the step of difference differentiation τ_T on the identification of the coefficient $a = 1.0$ according to algorithm I: lines 1 – $\tau_T = 0.0033$; 2 – $\tau_T = 0.0132$; 3 – a; 4 – a_0.

$\lambda_m(T)$ according to algorithm I depending on the magnitude of the step τ_T of the grid w_T (26) of numerical differentiation with respect to temperature in relation (13). Fig. 4 illustrates the dependence of the accuracy of the result on the choice of the point x_*. The calculations were carried out at the following parameters of calculation: $h_i = h = 0.005$, $i = 1,2,\ldots,N$, $\tau_t = 0.01$, $\tau_T = 37.0$, and $\varepsilon = 0.001$ (for the designations of the calculation parameters see Appendix A). Fig. 5 presents the results of simulation of $\lambda_m(T)$ according to algorithms II and III at the same (as in the case of algorithm I ($\tau_T = 10.0$)) parameters of computation and initial approximation.

We will compare the results of calculations according to algorithms I–III. These algorithms differ in the quality of reconstruction of the function $\lambda(T)$ at the edges of the segment $[T^{(1)}, T^{(2)}]$. For algorithm I the relations $\lambda_n(T^{(1)}) \simeq \lambda_0(T^{(1)})$, $\lambda_n(T^{(2)}) \simeq \lambda_0(T^{(2)})$ hold, where λ_0 is the initial approximation for $\lambda_n(T)$. Consequently, there is nonuniform estimation for $\lambda(T)$ in the vicinity of points $T^{(1)}, T^{(2)}$.

At the same time, calculations according to algorithm II make it possible in the vicinity of edge $T^{(2)}$ to approximate $\lambda_n(T)$ to the precise solution, whereas the use of relation (15) allows one to more precisely find $\lambda(T)$ in the vicinity of edge $T^{(1)}$. Here, both algorithms II and III possess a smoothing property, whereas algorithm I more precisely represents breakpoints of the plot of the function $\lambda(T)$.

Example 2. The proposed methods were tested also on a model example for an equation with constant coefficients:

$$\frac{\partial T}{\partial t} = a\frac{\partial^2 T}{\partial x^2}, \quad a > 0 - \text{const}. \tag{22}$$

As the solution of this equation we take the function

$$T = \frac{1}{2\sqrt{\pi a(t+c)}} \exp\left(-\frac{(x-d)^2}{4a(t+c)}\right). \tag{23}$$

Here, d, c – const, $c > 0$ are the parameters selected in a certain way and making it possible to change the character of solution behavior.

The values of the functions $g_1(t)$, $g_2(t)$, $\widetilde{T}(t)$, and $\overline{T}(x)$ are determined in accordance with the function (23). The nonlinear function $a_n(T)$ will be the result of the identification of the value of the coefficient a by the methods (9) and (10). We will present the results of numerical calculations at the following parameters of the model problem built: $b = 2.0$, $t_f = 2.0$, $d = 1.0$, $c = 0.3$, and $x_* = 1.0$. Fig. 6 shows the results of reconstruction according to algorithm I of the coefficient $a = 1.0$ at the initial approximation $a_0 = 1.5$ and in calculation with the parameters $h_i = h = 0.02$,

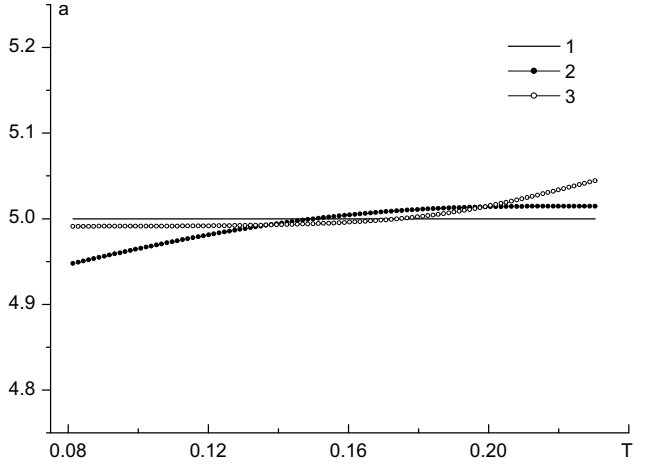

Fig. 7. Results of reconstruction of the coefficient $a = 5.0$: curve (1) according to algorithms II (2) and III (3).

$i = 1,2,\ldots,N$, $\tau_t = 0.001$, $\varepsilon = 10^{-11}$ and different steps τ_T of the temperature grid. Here, the numerical solution $T_n(x,t)$ of problem (22) obtained with the aid of the nonlinear coefficient an that corresponds to curve 2 (Fig. 6) virtually coincides with the exact solution (23): the inequality $\max_{0<i<N}|T_{n_i} - y_i| \leqslant 0.001$ holds. Fig. 7 presents the results of the reconstruction of the coefficient $a = 5.0$ at $a_0 = 4.0$ according to algorithms II and III. The parameters of calculations are $h_i = h = 0.02$, $i = 1,2,\ldots,N$, $\tau_t = 0.001$, $\tau_T = 0.0025$, and $\varepsilon = 10^{-11}$. In this case, the numerical solution of problem (22) by the constructed nonlinear coefficients is also close to precise solution (23). Note that in the vicinity of the values of $\widetilde{T}(t)$ the found approximate value of $a_n(T)$ virtually coincides with the precise value: $a_n(\widetilde{T}) \simeq 5.0$.

The results of computational experiments allow the conclusion that the choice of the gradient $J^i_{\lambda_n}$ $(i = 1,2,3)$ substantially influences the accuracy of results. In calculations according to algorithm I the nonuniformity of the identification of the thermal-conductivity coefficient is observed on the edges of the segment $[T^{(1)}, T^{(2)}]$ (see Fig. 6 (curve 1) and Fig. 8 (curves 1 and 2)). The calculations according to algorithm II yield a good result on the right edge of this segment (Fig. 7, curve 2), whereas calculations according to algorithm III – on the left edge (Fig. 7, curve 3).

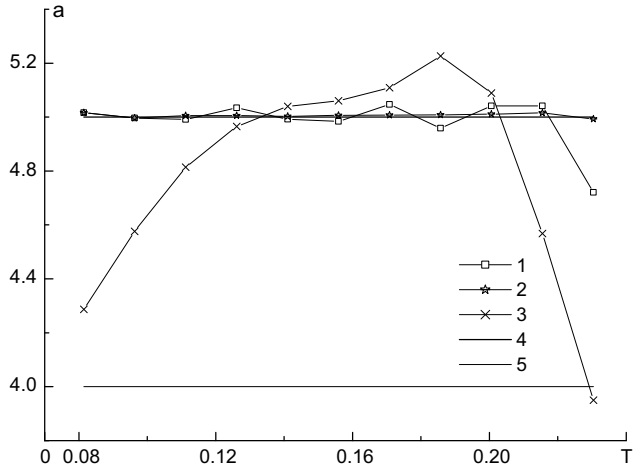

Fig. 8. Dynamics of reconstruction of the coefficient $a = 5.0$ according to algorithm I depending on the value of the discrepancy ε: lines 1 – $\varepsilon = 10^{-7}$, 2 – $\varepsilon = 10^{-11}$, 3 – $\varepsilon = 10^{-3}$, 4 – $a = 5$, and 5 – $a_0 = 4$.

The nonuniformity of the identification of the coefficient in the vicinity of the points $T^{(1)}$ and $T^{(2)}$ can be reduced on successful choice of the initial approximation, grid steps, tolerance, and of the point x_*.

The experiments carried out prove the substantial dependence of the accuracy of identification according to algorithm I on the choice of the step of numerical differentiation with respect to the temperature in (13). Use of a very small grid step ω_T in operation with gradient (13) may lead to the incipience of nonphysical oscillations and to a significant loss in accuracy, which can be seen in Fig. 3 (curve 3) and Fig. 6 (curve 1). Modeling of the reconstruction of the thermal-conductivity coefficient in operation with gradient (13) should be carried out in a large range of change of the grid step τ_T. However, in calculating the integrals in relations (14) and (15) the value of τ_T should be small enough.

The variation of the value of ε in (11) makes it possible to raise the accuracy of calculations. Fig. 8 demonstrates the influence of the value of ε on the result of identification according to algorithm I for Example 2. Here, with a change in ε from 10^{-3} to 10^{-11} the number of iterations in the iteration processes (9) and (10) changes from 1 ($\varepsilon = 10^{-3}$) to 70 ($\varepsilon = 10^{-11}$) (the remaining parameters correspond to the calculations presented in Fig. 7). However, it should be taken into account that the assignment of a very small value of ε may lead to an excessively great number of iteration cycles in the algorithms (9) and (10). Therefore, it is worthwhile to follow the rate of change in the tolerance and halt the iteration cycle in the case of a "slack" change of the tolerance.

Thus, various computational experiments have shown that in addition to the complex dependence of the real $\lambda(T)$ on temperature, the following basic factors influence the accuracy of the reconstruction of the coefficient: (1) the choice of the initial approximation $\lambda_0(T)$, (2) the form of the gradient $J^i_{\lambda n}$ $(i = 1, 2, 3)$ used for calculations (formulas (13)–(15)), (3) the value of the temperature measurement point x_*, (4) the selection of the grid steps ω_x, ω_t, ω_T, and (5) the value of ε in relation (11).

It is difficult to indicate a prior at least one of the indicated parameters which will yield a better result in the relationship between the accuracy and speed of calculations. Such a situation is typical on the whole of the problems of a nonlinear numerical analysis. The influence of the above-indicated factors on the accuracy and speed of calculations is usually of interrelated complex character.

5. Conclusions

The results of the investigations carried out show that the functional identification approach of the thermal-conductivity coefficient and its numerical algorithms are effective enough. To obtain satisfactory results of the reconstruction of $\lambda(T)$ over the entire segment $[T^{(1)}, T^{(2)}]$ due to the specific features of methods I, II, III near the boundaries of the segment investigated, it is worthwhile to compile the results of computations according to methods I, II, and III.

The proposed algorithms allow one to reconstruct the thermal-conductivity coefficient with a discontinuous derivative with respect to temperature at arbitrary, a priori unknown discontinuity points, which seems to be especially important in modeling coefficients for problems with phase changes.

Appendix A. Numerical algorithms

The construction of approximate algorithms for solving nonlinear unsteady-state boundary-value problems of mathematical physics 1,2,3, (16) and (20) is based on the difference method [18].

In the domain Ω, we introduce a nonuniform grid of nodes ω_x:

$$\omega_x = \left\{ x_i \in [0, b],\ x_i = x_0 + \sum_{k=1}^{i} h_k,\ i = 1, 2, \ldots, N,\ x_0 = 0,\ x_N = b \right\}, \tag{24}$$

and a uniform grid ω_t:

$$\omega_t = \{ t_j \in [0, t_f],\ t_j = \tau_t \cdot j,\ j = 0, 1, \ldots, j_0,\ t_{j_0} = t_f \}, \tag{25}$$

where x_i is the node of the grid ω_x, t_j is the node of the grid ω_t; h_i is the step of the grid ω_x, $i = 1, 2, \ldots, N$; $\hbar_i = 0.5(h_i + h_{i+1})$, $i = 1, 2, \ldots, N-1$; τ_t is the step of the grid ω_t, $\omega = \omega_x \times \omega_t$.

We construct the grid ω_x so that the point $x = x_*$ could be its node: $x_* = x_{i_*}, i_* \in \{2, 3, \ldots, N-2\}$.

Over the segment $[T^{(1)}, T^{(2)}]$ we introduce a uniform grid of nodes ω_T:

$$\omega_T = \Big\{ T_m \in [T^{(1)}, T^{(2)}],\ T_m = T_0 + \tau_T \cdot m, \quad m = 0, 1, \ldots, M,\ T_0 = T^{(1)},\ T_M = T^{(2)} \Big\}, \tag{26}$$

where τ_T is the step of the grid ω_T.

We introduce the notation. Let $y = y^j_i = y(x_i, t_j)$ be the function given on the grid ω, $i = 0, 1, \ldots, N$, $j = 0, 1, \ldots, j_0$. We define $y_x = (y^j_{i+1} - y^j_i)/h_{i+1}$, $i = 0, 1, 2, \ldots, N-1$, $y_{\bar{x}} = (y^j_{i+1} - y^j_i)/\hbar_i$, $i = 1, 2, \ldots, N-1$, $j = 0, 1, \ldots, j_0$; $y_{\bar{x}} = (y^j_i - y^j_{i-1})/h_i$, $i = 1, 2, \ldots, N$, $j = 0, 1, \ldots, j_0$; $\check{y} = y^{j-1}_i = y(x_i, t_{j-1})$, $y_{\bar{t}} = (y^j_i - y^{j-1}_i)/\tau_t$, $i = 0, 1, 2, \ldots, N$, $j = 1, 2, \ldots, j_0$.

For a certain grid operator $\Phi(y, \check{y})$ we assume that $\Phi(y, \check{y})|^j_i = \Phi(y^j_i, y^{j-1}_i)$, for example,

$$(y_{\bar{x}x} + c(\check{y})y_{\bar{t}})|^j_i = \frac{1}{\hbar_i}\left(\frac{y^j_{i+1} - y^j_i}{h_{i+1}} - \frac{y^j_i - y^j_{i-1}}{h_i} \right) + c(y^{j-1}_i)\frac{y^j_i - y^{j-1}_i}{\tau_t}.$$

For approximate solution of problems (1)–(3), we construct the difference scheme with weights

$$(\sigma c(y) + (1-\sigma)c(\check{y}))y_{\bar{t}}|^j_i = \sigma \Lambda(y)|^j_i + (1-\sigma)\Lambda(y)|^{j-1}_i,\ \sigma \in [0, 1], \quad i = 1, 2, \ldots, N-1,\ j = 1, 2, \ldots, j_0, \tag{27}$$

$$y^j_i = T(x_i), \quad i = 0, 1, 2, \ldots, N, \quad j = 0,$$
$$y^j_0 = g_1(t_j), \quad y^j_N = g_2(t_j), \quad j = 0, 1, 2, \ldots, j_0.$$

Here, y is the approximate value of T_n. The grid operator $\Lambda(y)|^j_i$ has the form

$$\Lambda y|_i^j = (a(y)y_{\bar{x}})_x|_i^j,$$

where $a_i^j(y) = 0.5(\lambda_n(y_{i-1}^j) + \lambda_n(y_i^j)),\ i = 1,2,\ldots,N, j = 0,1,\ldots,j_0$.

At $\sigma \neq 0$ the solution of the difference scheme (27) can be found with the aid of the following iteration process:

$$\left(\sigma c\left(\overset{s}{y}\right) + (1-\sigma)c(\check{y})\right)\frac{\overset{s+1}{y} - \check{y}}{\tau_t}\Bigg|_i^j = \left(\sigma(a(\overset{s}{y})\overset{s+1}{y}_{\bar{x}})_x + (1-\sigma)\Lambda\check{y}\right)\Bigg|_i^j,$$
$$i = 1,2,\ldots,N-1,\ j = 1,2,\ldots,j_0, \tag{28}$$

$$\overset{s+1}{y}{}_0^j = g_1(t_j), \qquad \overset{s+1}{y}{}_N^j = g_2(t_j), \quad j = 0,1,2,\ldots,j_0,$$

$s = 0,1,2,\ldots$ is the iteration number. For $s = 0$ and $\sigma = 1/2$, we assume that $\overset{s}{y}{}_i^j = 2y_i^{j-1} - y_i^{j-2},\ i = 1,2,\ldots,N-1,\ j = 2,3,\ldots,j_0$. For $j = 1$ and $s = 0$, we assume that $\overset{s}{y}{}_i^j = \overline{T}(x_i) + \tau_t(a(\overline{T})\overline{T}_{\bar{x}})_x|_i,\ i = 1,2,\ldots,N-1$. At $\sigma \neq 1/2$ for $s = 0$ we assume that $\overset{s}{y}{}_i^j = y_i^{j-1},\ i = 1,2,\ldots,N-1,\ j = 2,3,\ldots,j_0$.

The iteration is carried out till the fulfillment of the condition

$$\left|\overset{s+1}{y}_i - \overset{s}{y}_i\right| \leqslant \varepsilon_1\left|\overset{s}{y}_i\right| + \varepsilon_2, \quad i = 1,2,\ldots,N-1,$$

where ε_1 and ε_2 are the empirical parameters, $\varepsilon_1 = 0$ if $|\overset{s}{y}_i| \leqslant 1$ and $\varepsilon_2 = 0$ if $|\overset{s}{y}_i| > 1,\ i = 1,2,\ldots,N-1$. The finding of the values of $\overset{s+1}{y}_i\ (i = 0,1,\ldots,N)$ is reduced for each $s = 1,2,\ldots$ to the solution of the system of linear algebraic equations with a three-diagonal matrix. The solution of the system can be found with the aid of the pivot method [18].

At known values of $c(y),\ \lambda_n(y)$ the approximate values of the function w in problem (16) on the grid ω can be found from the difference relations

$$-((\sigma-1)c(y) + \sigma c(\check{y}))y_{\bar{t}}^*|_i^j = (\sigma-1)\lambda_n(y)y_{\bar{x}\hat{x}}^*\Big|_i^j + \sigma\lambda_n(y)y_{\bar{x}\hat{x}}^*\Big|_i^{j-1}$$
$$-f(x_i)\big((\sigma-1)p(t_j) + \sigma p(t_{j-1})\big); \quad i = 1,2,\ldots,N-1,$$
$$j = j_0, j_0-1,\ldots,1,$$

$$y_i^{*j_0} = 0, \quad i = 0,1,\ldots,N,$$

$$y_0^{*j} = y_N^{*j} = 0, \quad j = j_0, j_0-1,\ldots,1,0.$$

Here, y^* is the approximate value of w, the grid function $f(x_i)$ has the orm

$$f(x_i) = \begin{cases} 0.5/h_{i_*}, & i = i_*-1, i_*, i_*+1, \\ 0, & i = 1,\ldots,i_*-2; i_*+2, i_*+3,\ldots,N-1. \end{cases}$$

The solution of the problem constructed can be found successively for $j = j_0-1, j_0-2,\ldots,1,0$ with the aid of the pivot method at $\sigma \neq 0$ and from explicit formulas at $\sigma = 0$.

In solving numerically the problem (20), we assume that on the grid ω approximate grid values of $T_n(x_i,t_j)$ are known. We also assume that the grid values $c(y),\ \lambda_n(y),\ l_n(y)$ are known. The approximate value of problem (20) can be found on the grid ω with the aid of the difference scheme that is similar to (28):

$$\left(\frac{c(y)\tilde{y} - c(\check{y})\check{\tilde{y}}}{\tau_t}\right)\Bigg|_i^j = \sigma\left((\lambda_n(y)\tilde{y})_{\bar{x}\hat{x}} + (\tilde{a}(y)\tilde{y}_{\bar{x}})_{\hat{x}}\right)\Big|_i^j$$
$$+ (1-\sigma)\left((\lambda_n(y)y)_{\bar{x}\hat{x}} + (\tilde{a}(y)y_{\bar{x}})_{\hat{x}}\right)\Big|_i^{j-1},$$
$$i = 1,2,\ldots,N-1, \quad j = 1,2,\ldots,j_0,$$

$$\tilde{y}_i^j = 0, \quad j = 0, \quad i = 0,1,\ldots,N,$$

$$\tilde{y}_0^j = \tilde{y}_N^j = 0, \quad j = 1,2,\ldots,j_0.$$

Here, $\tilde{y}_i^j$ is the approximate value of $v(x_i,t_j),\ i = 0,1,2,\ldots,N,\ j = 0,1,\ldots,j_0$; $\tilde{a}(y)|_i^j = 0.5(l_n(y_{i-1}^j) + l_n(y_i^j)),\ i = 1,2,\ldots,N,\ j = 0,1,2,\ldots,j_0$.

The solution of the given difference problem at $j = 1,2,\ldots,j_0$ can be found directly by the pivot method, or ($\sigma = 0$) from recurrent relations.

References

[1] O.M. Alifanov, Inverse Heat Transfer Problems, Springer, Berlin, 1994.
[2] O.M. Alifanov, E.A. Artyukhin, C.V. Rumyantsev, Extreme Methods for Solving Ill-Posed Problems with Applications to Inverse Heat Transfer Problems, Begell House Inc., New York, 1995.
[3] E.A. Artyukhin, Thermal conductivity reconstruction from the solution of a nonlinear inverse problem, J. Eng. Phys. Thermophys. 41 (1981) 587–592.
[4] J.V. Beck, Nonlinear estimation applied to the nonlinear inverse heat conduction problem, Int. J. Heat Mass Transfer 13 (1970) 703–716.
[5] L.B. Dantas, H.R.B. Orlande, A function estimation approach for determining temperature-dependent thermophysical properties, Inverse Probl. Sci. Eng. 3 (1991) 201–279.
[6] A. Lorenzi, An inverse problem for semi-linear parabolic equation, Ann. Mat. Pura Appl. 31 (1982) 145–166.
[7] M.N. Özisik, N.R. Orlande, Inverse Heat Transfer: Fundamentals and Applications, Tailor & Francis, New York, 2000.
[8] H.R.B. Orlande, M.M. Özisik, Determination of the reaction function in reaction-diffusion parabolic problem, ASME J. Heat Transfer 116 (1984) 1040–1044.
[9] V.T. Borukhov, V.I. Timoshpolskii, Functional identification of the nonlinear thermal conductivity coefficient by gradient methods. I. Conjugate operators, J. Eng. Phys. Thermophys. 78 (2005) 695–702.
[10] V.T. Borukhov, V.I. Timoshpolskii, G.M. Zayats, V.A. Tsurko, Functional identification of the nonlinear thermal conductivity coefficient by gradient methods. II. Numerical modeling, J. Eng. Phys. Thermophys. 78 (2005) 703–709.
[11] P. DuChateau, R. Thelwell, G. Butters, Analysis of an adjoint problem approach to the identification of an unknown diffusion coefficient, Inverse Probl. 29 (2004) 601–625.
[12] J. Wang, A.J. Silva Neto, F.D. Moura Neto, J. Su, Function estimation with Alifanov's iterative regularization method in linear and nonlinear heat conduction, J. Appl. Math. Model. 26 (2002) 1093–1111.
[13] M.V. Klibanov, Global uniqueness of multidimensional inverse problem for a nonlinear parabolic equations by a Carleman estimate, Inverse Probl. 20 (2004) 1003–1032.
[14] M.V. Klibanov, A. Timonov, Carleman Estimates for Coefficient Inverse Problem and Numerical Application, VSP, Utrecht, 2004.
[15] C.V. Rumyantsev, Ways of regard to the a priori information in regularizing gradient algorithms, J. Eng. Phys. Thermophys. 49 (1985) 932–935.
[16] J.M. Matsevityi, A.V. Multanoviskii, Pointwise identification of thermophysical characteristics, J. Eng. Phys. Thermophys. 6 (1986) 1392–1397.
[17] A.D. Polyanin, V.F. Zaitsev, A.I. Zhurov, Methods of solving nonlinear equations of the mathematical physics and mechanics, Izd. Fizmatlit (2005).
[18] A.A. Samarskii, The Theory of Difference Schemes, CRC Press, Boca Raton, FL, 2001.
[19] V.I. Krylov, Approximate Calculation of Integrals, Macmillan, London, 1962.